Higher-order non-linear effects for optical lattice clocks on Mg atoms

V.D. Ovsiannikov, S.I. Marmo, S.N. Mokhnenko

Voronezh State University, 394006 Voronezh, Russia

and V.G. Palchikov

FGUP "VNIIFTRI", 141570 Mendeleevo, Moscow Region,
National Research Nuclear University "MEPhI", Moscow, Russia

Email: ovd@phys.vsu.ru

Новосибирск, Физика ультрахолодных атомов, Декабрь -2016

1. INTRODUCTION

Motivation:

High-precision measurement of the magic wavelength for an optical lattice

$$\lambda_{mag} = 468.46\ \mathrm{nm}$$

of a clock based on the frequency of a strongly forbidden transition of Mg atom between metastable 3s3p($^3P_0$) and ground $3s^2$ ($^1S_0$) states reported in the paper

A.P. Kulosa, D. Fim, K.H. Zipfel, S. Rühmann, S. Sauer, N. Jha, K. Gibble, W. Ertmer, E.M. Rasel, M.S. Safronova, U.I. Safronova, and S.G. Porsev "Towards a Mg lattice clock: observation of the 1S0−3P0 transition and determination of the magic wavelength", Phys.Rev.Lett. vol. **115**, 240801 (2015).

PHYSICAL REVIEW A **88**, 013405 (2013)

Multipole, nonlinear, and anharmonic uncertainties of clocks of Sr atoms in an optical lattice

V. D. Ovsiannikov
Physics Department, Voronezh State University, Voronezh 394006, Russia

V. G. Pal'chikov
Institute of Metrology for Time and Space at National Research Institute for Physical-Technical and Radiotechnical Measurements, Mendeleevo, Moscow Region, 141579, Russia

A. V. Taichenachev and V. I. Yudin
Institute of Laser Physics SB RAS, pr. Ac. Lavrentyeva, 13/3, Novosibirsk, 630090 Russia, Novosibirsk State University, ul. Pirogova, 2, Novosibirsk, 630090, Russia, Novosibirsk State Technical University, pr. K. Marksa, 20, Novosibirsk, 630073, Russia, and Russian Quantum Center, Skolkovo, Moscow Reg., 143025, Russia

Hidetoshi Katori
Department of Applied Physics, Graduate School of Engineering, The University of Tokyo, Bunkyo-ku, Tokyo 113-8656, Japan, Innovative Space-Time Project, ERATO, Japan Science and Technology Agency, Bunkyo-ku, Tokyo 113-8656, Japan and Quantum Metrology Laboratory, RIKEN, Wako-shi, Saitama 351-0198, Japan

(Received 19 April 2013; published 8 July 2013)

Magnetic-dipole, electric-quadrupole, and hyperpolarizability effects on clock energy levels are analyzed in detail for Sr atoms in Stark potentials of red-detuned and blue-detuned magic-wavelength optical lattices. A difference between ac Stark shifts in traveling and standing waves is determined numerically. Differences between magic wavelengths for atoms in traveling and standing waves are presented and strategies for minimizing uncertainties of the clock frequency are indicated explicitly. Significant suppression of hyperpolarizability effect is demonstrated analytically for a blue-detuned in comparison with a red-detuned lattice, thus enabling essential deepening of trap potentials, reducing tunneling between lattice wells and collision effects.

PHYSICAL REVIEW A **91**, 052503 (2015)

Strategies for reducing the light shift in atomic clocks

Hidetoshi Katori*
Department of Applied Physics, Graduate School of Engineering, The University of Tokyo, Bunkyo-ku, Tokyo 113-8656, Japan; Innovative Space-Time Project, ERATO, Japan Science and Technology Agency, Bunkyo-ku, Tokyo 113-8656, Japan; and Quantum Metrology Laboratory, RIKEN, Wako-shi, Saitama 351-0198, Japan

V. D. Ovsiannikov† and S. I. Marmo
Department of Physics, Voronezh State University, 394006 Voronezh, Russia

V. G. Palchikov
FGUP VNIIFTRI, 141570 Mendeleevo, Moscow Region, Russia and National Research Nuclear University "MEPhI," Moscow, Russia

(Received 20 December 2014; published 14 May 2015)

Recent progress in optical lattice clocks requires unprecedented precision in controlling systematic uncertainties at the 10^{-18} level. Tuning of nonlinear light shifts is shown to reduce lattice-induced clock shift for a wide range of lattice intensity. Based on theoretical multipolar, nonlinear, anharmonic, and higher-order light shifts, we numerically demonstrate possible strategies for Sr, Yb, and Hg clocks to achieve lattice-induced systematic uncertainty below 1×10^{-18}.

DOI: 10.1103/PhysRevA.91.052503 PACS number(s): 32.70.Jz, 06.30.Ft, 37.10.Jk, 42.62.Eh

I. INTRODUCTION

The last few years have witnessed significant advances in optical clocks to reach uncertainties of the 10^{-18} level in ion-based clocks [1] and optical lattice clocks [2,3]. Hitherto unexplored accuracy of optical clocks opens up new possibilities in science and technologies, such as probing new physics via possible variation of fundamental constants [4–6], and relativistic geodesy to measure gravitational potential differences [1]. Evaluations of perturbations on the clock transitions are indeed at the heart of these endeavors.

Unperturbed transition frequencies have been accessed by extrapolating perturbations to zero, which is straightforward and light-polarization-dependent hyperpolarizability effect [18] can be used to tailor the intensity dependence of light shifts. We define an "operational magic frequency" to reduce light shift to less than 1×10^{-18} for a sufficiently larger intensity variation than is necessary for confining atoms. Numerical calculations for electric-dipole ($E1$), magnetic-dipole ($M1$), and electric-quadrupole ($E2$) polarizabilities and hyperpolarizabilities are presented for the ${}^1S_0$-${}^3P_0$ clock transitions in Sr, Yb, and Hg atoms, which are used to demonstrate the feasibility of the proposed strategies.

II. LATTICE-INDUCED LIGHT SHIFTS

PHYSICAL REVIEW A **93**, 043420 (2016)

Higher-order effects on the precision of clocks of neutral atoms in optical lattices

V. D. Ovsiannikov* and S. I. Marmo
Voronezh State University, 394006 Voronezh, Russia

V. G. Palchikov
FGUP "VNIIFTRI," 141570 Mendeleevo, Moscow Region, Russia
and National Research Nuclear University "MEPhI," Moscow, Russia

H. Katori
Department of Applied Physics, Graduate School of Engineering, The University of Tokyo, Bunkyo-ku, Tokyo, 113–8656, Japan;
Innovative Space-Time Project ERATO, Japan Science and Technology Agency, Bunkyo-ku,Tokyo, 113–8656, Japan;
and Quantum Metrology Laboratory, RIKEN, Wako-shi, Saitama 351-0198, Japan
(Received 9 February 2016; published 26 April 2016)

The recent progress in designing optical lattice clocks with fractional uncertainties below 10^{-17} requires unprecedented precision in estimating the role of higher-order effects of atom-lattice interactions. In this paper, we present results of systematic theoretical evaluations of the multipole, nonlinear, and anharmonic effects on the optical-lattice-based clocks of alkaline-earth-like atoms. Modifications of the model-potential approach are introduced to minimize discrepancies of theoretical evaluations from the most reliable experimental data. Dipole polarizabilities, hyperpolarizabilities, and multipolar polarizabilities for neutral Ca, Sr, Yb, Zn, Cd, and Hg atoms are calculated in the modified approach.

PERIODIC TABLE

Atomic Properties of the Elements

NIST

National Institute of Standards and Technology
Technology Administration, U.S. Department of Commerce

Physics Laboratory
physics.nist.gov

Standard Reference Data Group
www.nist.gov/srd

Frequently used fundamental physical constants

For the most accurate values of these and other constants, visit physics.nist.gov/constants

1 second = 9 192 631 770 periods of radiation corresponding to the transition between the two hyperfine levels of the ground state of ^{133}Cs

speed of light in vacuum	c	$299\ 792\ 458\ \mathrm{m\ s^{-1}}$	(exact)
Planck constant	h	$6.6261 \times 10^{-34}\ \mathrm{J\ s}$	$(\hbar = h/2\pi)$
elementary charge	e	$1.6022 \times 10^{-19}\ \mathrm{C}$	
electron mass	m_e	$9.1094 \times 10^{-31}\ \mathrm{kg}$	
	$m_e c^2$	$0.5110\ \mathrm{MeV}$	
proton mass	m_p	$1.6726 \times 10^{-27}\ \mathrm{kg}$	
fine-structure constant	α	$1/137.036$	
Rydberg constant	R_∞	$10\ 973\ 732\ \mathrm{m^{-1}}$	
	$R_\infty c$	$3.289\ 842 \times 10^{15}\ \mathrm{Hz}$	
	$R_\infty hc$	$13.6057\ \mathrm{eV}$	
Boltzmann constant	k	$1.3807 \times 10^{-23}\ \mathrm{J\ K^{-1}}$	

Solids
Liquids
Gases
Artificially Prepared

Period	1 IA	2 IIA	3 IIIB	4 IVB	5 VB	6 VIB	7 VIIB	8 VIII	9 VIII	10 VIII	11 IB	12 IIB	13 IIIA	14 IVA	15 VA	16 VIA	17 VIIA	18 VIIIA
1	1 H Hydrogen 1.00794																	2 He Helium 4.002602
2	3 Li Lithium 6.941	4 Be Beryllium 9.012182											5 B Boron 10.811	6 C Carbon 12.0107	7 N Nitrogen 14.0067	8 O Oxygen 15.9994	9 F Fluorine 18.9984032	10 Ne Neon 20.1797
3	11 Na Sodium 22.989770	12 Mg Magnesium 24.3050											13 Al Aluminum 26.981538	14 Si Silicon 28.0855	15 P Phosphorus 30.973761	16 S Sulfur 32.065	17 Cl Chlorine 35.453	18 Ar Argon 39.948
4	19 K Potassium 39.0983	20 Ca Calcium 40.078	21 Sc Scandium 44.955910	22 Ti Titanium 47.867	23 V Vanadium 50.9415	24 Cr Chromium 51.9961	25 Mn Manganese 54.938049	26 Fe Iron 55.845	27 Co Cobalt 58.933200	28 Ni Nickel 58.6934	29 Cu Copper 63.546	30 Zn Zinc 65.409	31 Ga Gallium 69.723	32 Ge Germanium 72.64	33 As Arsenic 74.92160	34 Se Selenium 78.96	35 Br Bromine 79.904	36 Kr Krypton 83.798
5	37 Rb Rubidium 85.4678	38 Sr Strontium 87.62	39 Y Yttrium 88.90585	40 Zr Zirconium 91.224	41 Nb Niobium 92.90638	42 Mo Molybdenum 95.94	43 Tc Technetium (98)	44 Ru Ruthenium 101.07	45 Rh Rhodium 102.90550	46 Pd Palladium 106.42	47 Ag Silver 107.8682	48 Cd Cadmium 112.411	49 In Indium 114.818	50 Sn Tin 118.710	51 Sb Antimony 121.760	52 Te Tellurium 127.60	53 I Iodine 126.90447	54 Xe Xenon 131.293
6	55 Cs Cesium 132.90545	56 Ba Barium 137.327		72 Hf Hafnium 178.49	73 Ta Tantalum 180.9479	74 W Tungsten 183.84	75 Re Rhenium 186.207	76 Os Osmium 190.23	77 Ir Iridium 192.217	78 Pt Platinum 195.078	79 Au Gold 196.96655	80 Hg Mercury 200.59	81 Tl Thallium 204.3833	82 Pb Lead 207.2	83 Bi Bismuth 208.98038	84 Po Polonium (209)	85 At Astatine (210)	86 Rn Radon (222)
7	87 Fr Francium (223)	88 Ra Radium (226)		104 Rf Rutherfordium (261)	105 Db Dubnium (262)	106 Sg Seaborgium (266)	107 Bh Bohrium (264)	108 Hs Hassium (277)	109 Mt Meitnerium (268)	110 Uun Ununnilium (281)	111 Uuu Unununium (272)	112 Uub Ununbium (285)		114 Uuq Ununquadium (289)		116 Uuh Ununhexium (292)		

Lanthanides	57 La Lanthanum 138.9055	58 Ce Cerium 140.116	59 Pr Praseodymium 140.90765	60 Nd Neodymium 144.24	61 Pm Promethium (145)	62 Sm Samarium 150.36	63 Eu Europium 151.964	64 Gd Gadolinium 157.25	65 Tb Terbium 158.92534	66 Dy Dysprosium 162.500	67 Ho Holmium 164.93032	68 Er Erbium 167.259	69 Tm Thulium 168.93421	70 Yb Ytterbium 173.04	71 Lu Lutetium 174.967
Actinides	89 Ac Actinium (227)	90 Th Thorium 232.0381	91 Pa Protactinium 231.03588	92 U Uranium 238.02891	93 Np Neptunium (237)	94 Pu Plutonium (244)	95 Am Americium (243)	96 Cm Curium (247)	97 Bk Berkelium (247)	98 Cf Californium (251)	99 Es Einsteinium (252)	100 Fm Fermium (257)	101 Md Mendelevium (258)	102 No Nobelium (259)	103 Lr Lawrencium (262)

Key: Atomic Number (58), Ground-state Level ($^1G^\circ_4$), Symbol (Ce), Name (Cerium), Atomic Weight† (140.116), Ground-state Configuration ([Xe]4f5d6s²), Ionization Energy (eV) (5.5387)

†Based upon ^{12}C. () indicates the mass number of the most stable isotope.

For a description of the data, visit physics.nist.gov/data

NIST SP 966 (September 2003)

Совершенствование эталонов времени. Достижения лучших лабораторий мира.

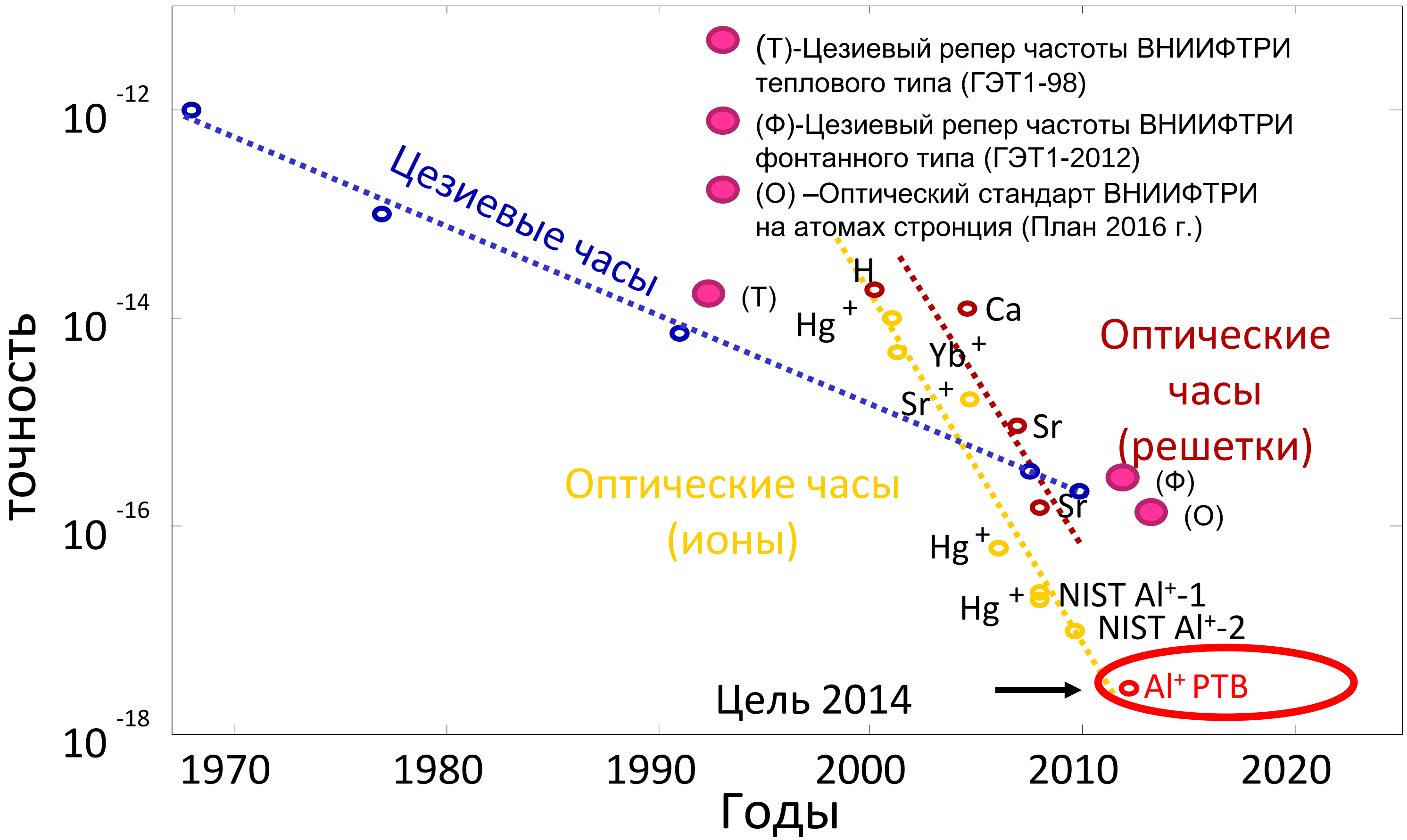

Cold-atom clocks: what for ?

- **Cold-atom clock development has made excellent progress**
  - Cold Cs microwave clock (uncertainty ~ 2 x 10^{-16})
  - Cold atom/ion clocks (unc. as low as 6 x 10^{-18}, instability ~ 1 x 10^{-18})

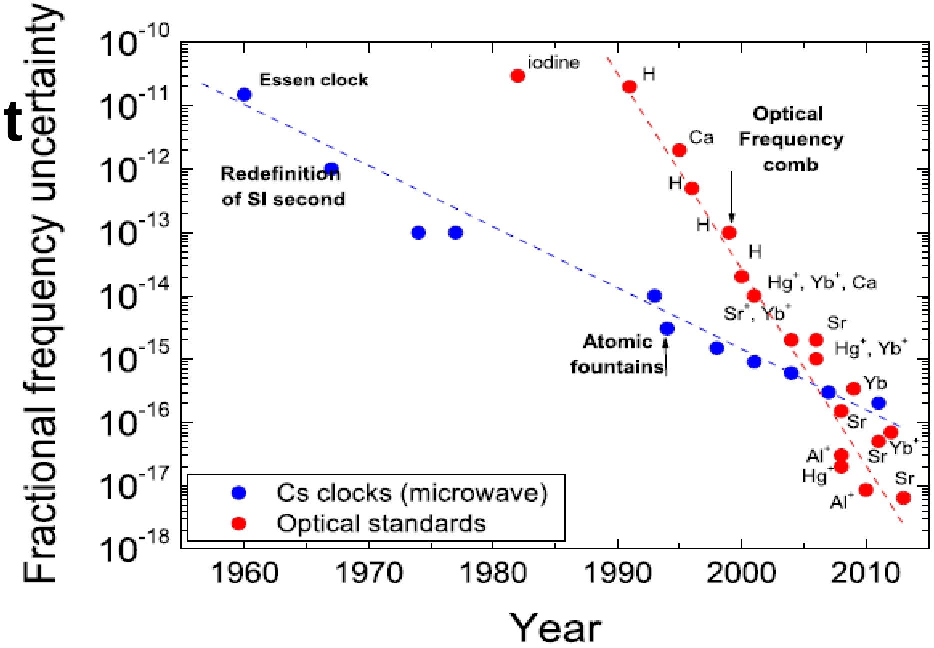

- **Scientific applications**
  - „Physics of clocks“
  - Tests of the Equivalence Principle (on the ground, laboratory experiments)
  - Tests of General Relativity (structure of space-time) → **space missions**
  - Geophysics: determination of the geopotential
  - Radio science
- **Technical applications** (spacecraft navigation in deep space: clocks/oscillators operated at deep space antenna sites)

PUBLIC RELEASE: 28-NOV-2016

NIST debuts dual atomic clock -- and a new stability record

NATIONAL INSTITUTE OF STANDARDS AND TECHNOLOGY (NIST)

SHARE PRINT E-MAIL

Media Contact

Laura Ost
laura.ost@nist.gov

@usnistgov

http://www.nist.gov

More on this News Release

NIST debuts dual atomic clock -- and a new stability record

NATIONAL INSTITUTE OF STANDARDS AND TECHNOLOGY (NIST)

JOURNAL
Nature Photonics

FUNDER
Defense Advanced Research Projects Agency, NASA

KEYWORDS

Излучение черного тела

Typical structure of energy levels in alkaline-earth and alkaline-earth-like atoms (Mg, Ca, Sr, Zn, Cd, Hg, Yb)

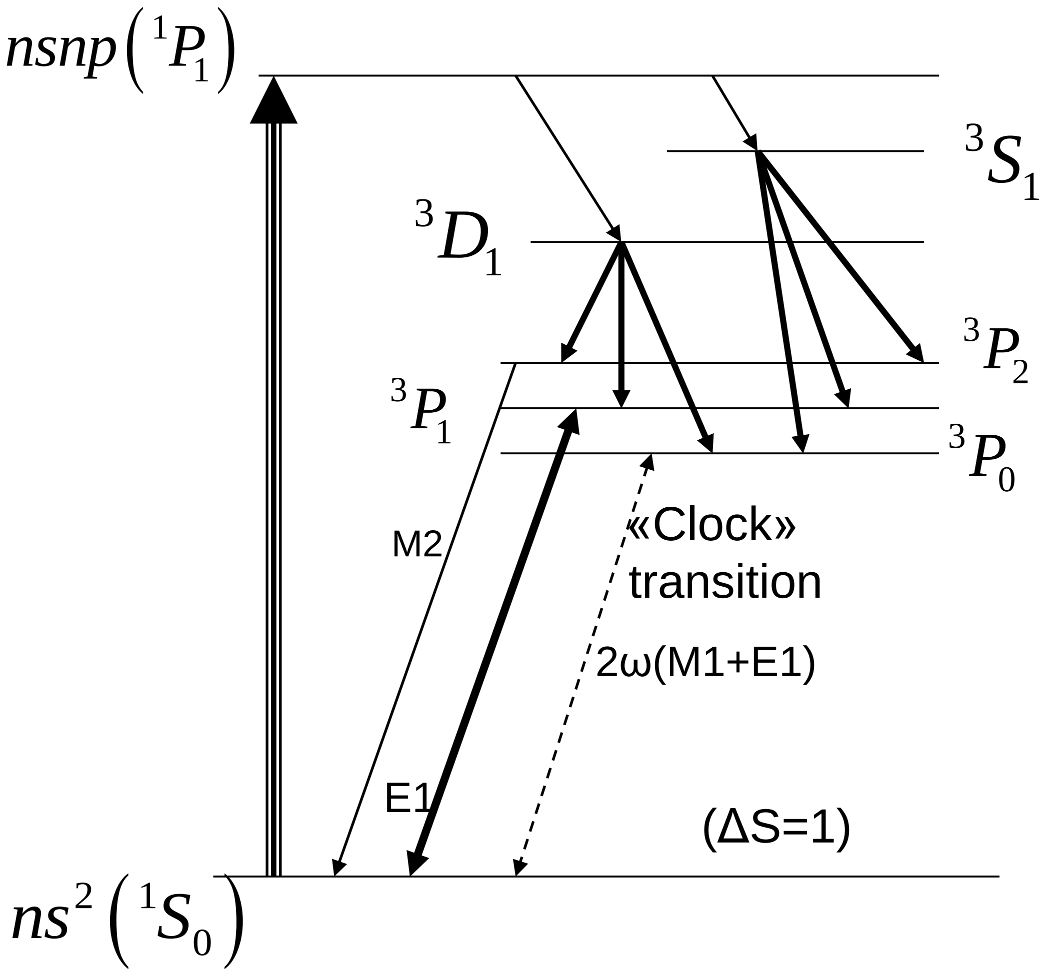

Radiation transition between metastable and ground states, stimulated in odd isotopes by the hyperfine interaction, is strictly forbidden in even isotopes.

This restriction makes extremely narrow the line of the clock transition, ${}^3P_0 - {}^1S_0$ **which may be stimulated by an external magnetic field or by the circularly polarized lattice wave. This transition may be used as an oscillator with extremely high quality**

$$Q = \nu_{cl} / \gamma > 10^{17}$$

The width γ **of the oscillator depends on (and may be regulated by) the intensity of the lattice wave or the magnetic field.**

Natural isotope composition

Even isotopes (I=0)	abundance	Odd isotopes abundance	($I\neq0$)
^{24,26}Mg:	90%	^{25}Mg: 10%	(I=5/2)
$^{40\rightarrow48}$Ca:	98.7%	^{43}Ca: 1.3%	(I=7/2)
^{84,86,88}Sr:	93%	^{87}Sr: 7%	(I=9/2)

==

$^{64\rightarrow70}$Zn:	95.9%	^{67}Zn: 4.1%	(I=5/2)
$^{106\rightarrow116}$Cd:	75%	^{111,113}Cd: 25%	(I=1/2)
$^{196\rightarrow204}$Hg:	69.8%	^{199,201}Hg: 30.2%	(I=1/2,3/2)

==

$^{168\rightarrow176}$Yb:	73%	^{171,173}Yb: 27%	(I=1/2, 5/2)

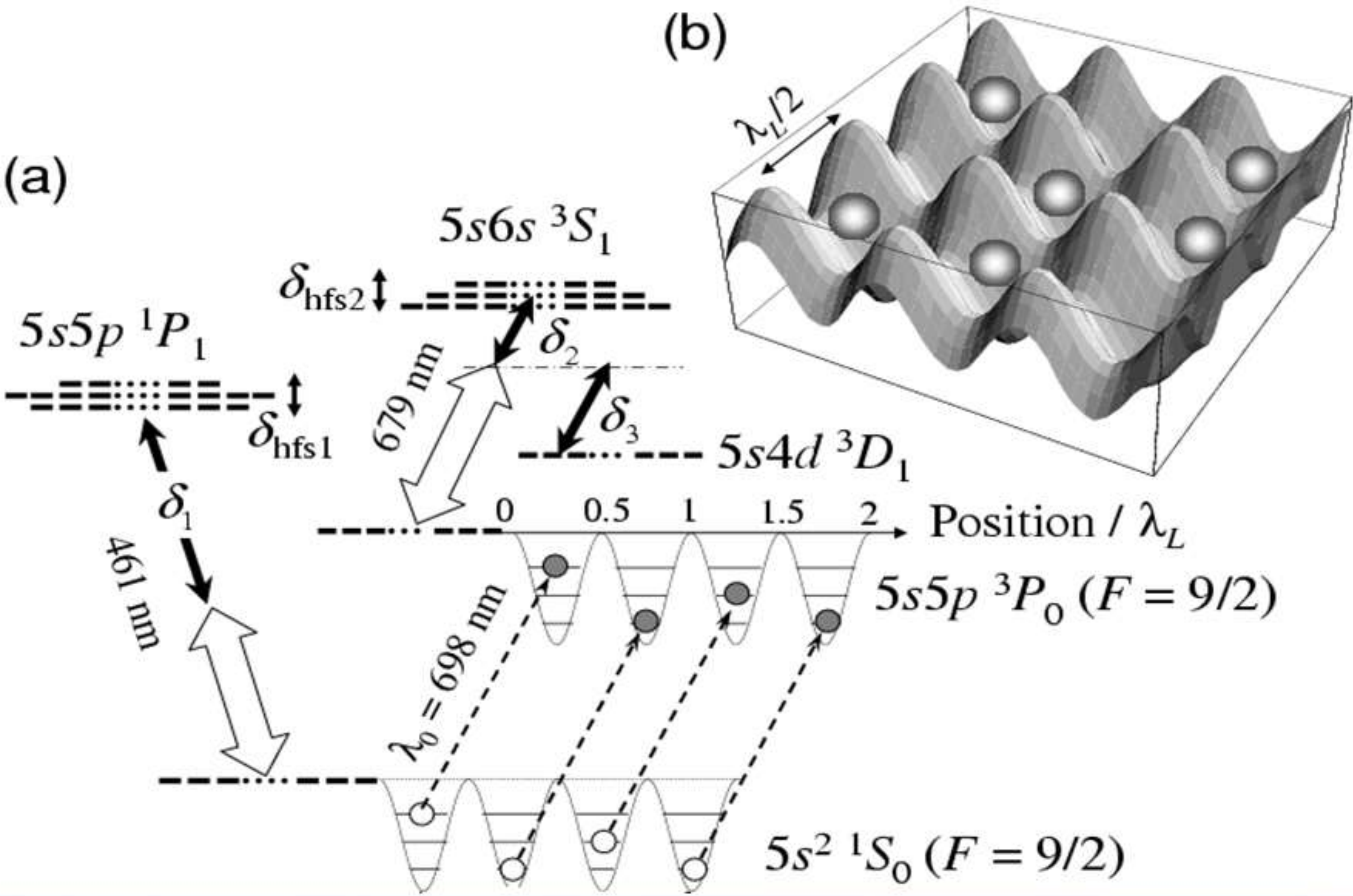

Simplified optical coupling scheme for Sr(87). From (H.Katori, M.Takamoto, V.G.Pal'chikov, V.D.Ovsiannikov, PRL ,Vol.91, 173005(2003)

Summary for higher-order contributions for Sr atoms

- **1. Polarizabilities.** To calculate the M1 and E2 contributions to the polarizability α, the magnetic dipole and electric quadrupole atom-field interactions should be taken into account together with the electric-dipole terms.
- Numerical estimates with the frequency ω, which $\alpha(\omega)=0$ gives
- α (M1)$\approx \alpha$ (E2) $\approx$10^(-7) $\times\alpha$ (E1) (H.Katori, M.Takamoto, Pal'chikov et al, PRL, 2003)
- **2. Hyperpolarizabilities.** Hyperpolarizabilities of the clock states at ω, which $\alpha(\omega)=0$, are:
- β (1S0)=6.3$\times$10^6 a.u.
- β (3P0)=2.7$\times$10^8 a.u.
- The relative contribution due to hyperpolarizabilities for the light shift is about $\approx$5$\times$10^-18
- at intensity 10 kW/cm^2
- **3. Anticrossing effect** .
- Off-diagonal matrix element is not zero:
- <3P0! H(2)!3P2>$\approx$-α(tensor) a.u.
- A.Derevianko, W.Johnson, V.Pal'chikov et al, PRA, 1999
- **4. Spin-Spin mixing effect** is very small
- (V.Pal'chikov, G.von Oppen, JETP, 1999; Physica Scripta, 1998)
- 5**. Measurement** for the magic wavelength:
- λ = 813.4 nm (H.Katori et al, Nature, 2005, 435, 321)
- and frequency 429 228 004 229 875.3(3.8) Hz(H.Katory et al,J.Phys.Soc,Jpn, 2006)
- 6. **Theory** for the magic wavelength:
- λ = 808.9 nm (in press)
- 7. **BBR effect**. $\delta\nu$ (BBR)/ ν(0) $\cong$-5.5$\times$10^(-15)
- A.Derevianko and S.Porsev (to be published)

General formulations for ac Stark effect

Finally, the light shift may be expressed in a form

$$\hbar\nu = \hbar\nu^{(0)} - \frac{1}{4}\Delta\alpha(\vec{e},\omega)I - \frac{1}{64}\Delta\gamma(\vec{e},\omega)I^2..,$$

Depending on the frequency and polarization of the laser field .

$$\vec{F}(t) = F\,\mathrm{Re}\left\{\vec{e}\exp\left[(\vec{k}\cdot\vec{r} - \omega t)\right]\right\}$$

1. **N.L. Manakov, V.D. Ovsiannikov, and L.P. Rapoport, *Phys. Reports* 141, 319(1986).**

$$\hbar\nu = \hbar\nu^{(0)} - \frac{1}{4}\Delta\alpha(\vec{e},\omega)I - \Delta\beta(\vec{e},\omega)\sqrt{I} - \frac{1}{64}\Delta\gamma(\vec{e},\omega)I^2..,$$

The term $\propto I^{1/2}$ was first predicted in [A.Taichenachev et al, PRL, 101, 193601(2008)]

2. Optical lattice

As follows from the Maxwell's equations,

$$\text{rot}\,\mathbf{E} = -\frac{1}{c}\frac{\partial \mathbf{B}}{\partial t}, \quad \text{rot}\,\mathbf{B} = \frac{1}{c}\frac{\partial \mathbf{E}}{\partial t},$$

electric- and magnetic-field vectors in a traveling wave are on-phase

$$\mathbf{E}^t_{\pm}(X,t) = \mathbf{E}_0 \cos(\pm kX - \omega t), \quad \mathbf{k} = \mathbf{e}_X k, \quad k = \omega / c = 2\pi / \lambda;$$

$$\mathbf{B}^t_{\pm}(X,t) = \mathbf{B}^t_{0\pm} \cos(\pm kX - \omega t), \quad \mathbf{B}^t_{0\pm} = \pm\left[\mathbf{e}_X \times \mathbf{E}_0\right].$$

Mean temporal distributions of electric- and magnetic-field energies in a traveling wave are space-uniform (independent of position)

<u>instantaneous</u> <u>mean temporal and spatial</u>

$$w^t_{\pm} = \frac{(\mathbf{E}^t_{\pm})^2 + (\mathbf{B}^t_{\pm})^2}{8\pi} = \frac{(\mathbf{E}_0)^2}{4\pi}\cos^2(\pm kX - \omega t); \qquad \overline{w^t_{\pm}} = \left\langle w^t_{\pm} \right\rangle = \frac{(\mathbf{E}_0)^2}{8\pi}$$

Electric- and magnetic-field vectors in a standing wave are a quarter-period off-phase

$$\mathbf{E}^s(X,t) = \mathbf{E}_+^t(X,t) + \mathbf{E}_-^t(X,t) = \mathbf{E}_0^s \cos(kX)\cos(\omega t), \quad \mathbf{E}_0^s = 2\mathbf{E}_{0\pm},$$

$$\mathbf{B}^s(X,t) = \mathbf{B}_+^t(X,t) + \mathbf{B}_-^t(X,t) = \mathbf{B}_0^s \sin(kX)\sin(\omega t), \quad \mathbf{B}_0^s = 2\mathbf{B}_{0\pm}^t.$$

Therefore, the mean temporal distributions of electric- and magnetic-field energies in a standing wave are space-dependent and also a quarter-period off-phase

<u>instantaneous</u> | <u>mean temporal</u>

$$w_E^s(X,t) = \frac{\left(\mathbf{E}^s(X,t)\right)^2}{8\pi} = \frac{(\mathbf{E}_0)^2}{2\pi}\cos^2(kX)\cos^2(\omega t); \qquad \overline{w_E^s} = \frac{(\mathbf{E}_0)^2}{4\pi}\cos^2(kX)$$

$$w_B^s(X,t) = \frac{\left(\mathbf{B}^s(X,t)\right)^2}{8\pi} = \frac{(\mathbf{B}_0)^2}{2\pi}\sin^2(kX)\sin^2(\omega t); \qquad \overline{w_B^s} = \frac{(\mathbf{E}_0)^2}{4\pi}\sin^2(kX)$$

2a) Spatial distribution of atom-lattice interaction

$$\mathbf{E}(X,t) = 2\mathbf{E}_0 \cos(kX)\cos(\omega t), \qquad k = \frac{\omega}{c} = \frac{2\pi}{\lambda}$$

$$\hat{V}(X,t) = \mathrm{Re}\left\{\hat{V}(X)\exp(-i\omega t)\right\}$$

$$\hat{V}(X) = \hat{V}_{E1}\cos(kX) + (\hat{V}_{E2} + \hat{V}_{M1})\sin(kX)$$

$$\hat{V}_{E1} = (\mathbf{r}\cdot\mathbf{E}_0); \quad \hat{V}_{E2} = \frac{\alpha\omega}{\sqrt{6}} r^2 \left(\left\{\mathbf{E}_0 \otimes \mathbf{n}\right\}_2 \cdot \mathbf{C}_2(\theta,\varphi)\right); \quad \hat{V}_{M1} = \frac{\alpha}{2}\left([\mathbf{n}\times\mathbf{E}_0]\cdot(\hat{\mathbf{J}} + \hat{\mathbf{S}})\right);$$

$$\mathbf{r} = r\mathbf{n}, \quad |\mathbf{n}| = 1.$$

The Stark-effect energy shift induced by the atom-lattice interaction is

$$\Delta E^{latt}_{g(e)}(X) = E^{(2)}_{g(e)}(X) + E^{(4)}_{g(e)}(X) + \ldots$$

$$E^{(2)}_{g(e)}(X) = -\left\langle g(e) \middle| \hat{V}^{\dagger}(X) G^{\omega} \hat{V}(X) + \hat{V}(X) G^{-\omega} \hat{V}^{\dagger}(X) \middle| g(e) \right\rangle =$$
$$= -\left\{ \alpha^{E1}_{g(e)}(\omega) \cos^2(kX) + \alpha^{qm}_{g(e)}(\omega) \sin^2(kX) \right\} I$$

where $\alpha^{E1}_{g(e)}(\omega)$ is the dipole polarizability; G^{E}, the Green's function.

$\alpha^{qm}_{g(e)}(\omega) = \alpha^{E2}_{g(e)}(\omega) + \alpha^{M1}_{g(e)}(\omega)$ is the multipole polarizability;

$I = cE_0^2/8\pi$ is the mean intensity of an input laser beam

$$E^{(4)}_{g(e)}(X) = -\beta_{g(e)}(\omega) \cos^4(kX) I^2.$$

2b) Lattice potential wells.

The clock-level shift is the lattice-trap potential energy, which consists of the wells separated *π/k=λ/2* from each other. Atoms locate near their equilibrium positions at the well bottoms. Assuming the departure of atom from the bottom *X<<1/k = λ/2π, the* energy of atom-lattice interaction may be presented, as follows

$$\Delta E^{latt}_{g(e)}(X) = U^{latt}_{g(e)}(X) \approx -D_{g(e)} + U^{(harm)}_{g(e)} X^2 - U^{(anh)}_{g(e)} X^4;$$

$$D_{g(e)}(\omega,\xi,I) = \alpha^{E1}_{g(e)}(\omega) I + \beta_{g(e)}(\xi,\omega) I^2, \quad - \text{ depth}$$

$$U^{(harm)}_{g(e)} = \left[\alpha^{dqm}_{g(e)}(\omega) I + 2\beta_{g(e)}(\xi,\omega) I^2\right] k^2 = \frac{M_{at}\Omega^2(\omega,\xi,I)}{2},$$

$$U^{(anh)}_{g(e)}(\omega,\xi,I) = \left[\alpha^{dqm}_{g(e)}(\omega) I + 5\beta_{g(e)}(\xi,\omega) I^2\right] \frac{k^4}{3}$$

$$\alpha^{dqm}_{g(e)}(\omega) = \alpha^{E1}_{g(e)}(\omega) - \alpha^{qm}_{g(e)}(\omega)$$

The clock-level energies include the energies $\mathrm{E}_{g(e)}^{vib}$ of atomic motion in the lattice well, determined from the Schrödinger equation

$$\hat{\mathrm{H}}_{g(e)}^{at}(X)\Psi_n(X)=\mathrm{E}_{g(e)}^{vib}\Psi_n(X)$$ of the Hamiltonian

$$\hat{\mathrm{H}}_{g(e)}^{at}(X)=\frac{\hat{\mathrm{P}}_{\mathrm{at}}^2}{2\mathrm{M}_{\mathrm{at}}}+U_{g(e)}^{latt}(X),\quad \hat{\mathrm{P}}_{\mathrm{at}}=-i\frac{\partial}{\partial X};$$

$$\mathrm{E}_{g(e)}^{vib}(\omega,\xi,I,n)=\underbrace{-D_{g(e)}(\omega,\xi,I)}_{depth}+\underbrace{\Omega_{g(e)}(\omega,\xi,I)\left(n+\frac{1}{2}\right)}_{harmonic\ oscillations}-\underbrace{\mathrm{E}_{g(e)}^{anh}(\omega,\xi,I)\left(n^2+n+\frac{1}{2}\right)}_{anharmonic\ energy}$$

$$\mathrm{E}_{g(e)}^{anh}(\omega,\xi,I)=\frac{\mathrm{E}^{rec}}{2}\left[1+\frac{3\beta_{g(e)}(\xi,\omega)I}{\alpha_{g(e)}^{dqm}(\omega)}\right];$$

$$\mathrm{E}_t^{rec}=\frac{\omega^2}{2\mathrm{M}_{\mathrm{at}}c^2}$$ is the recoil energy of a lattice photon

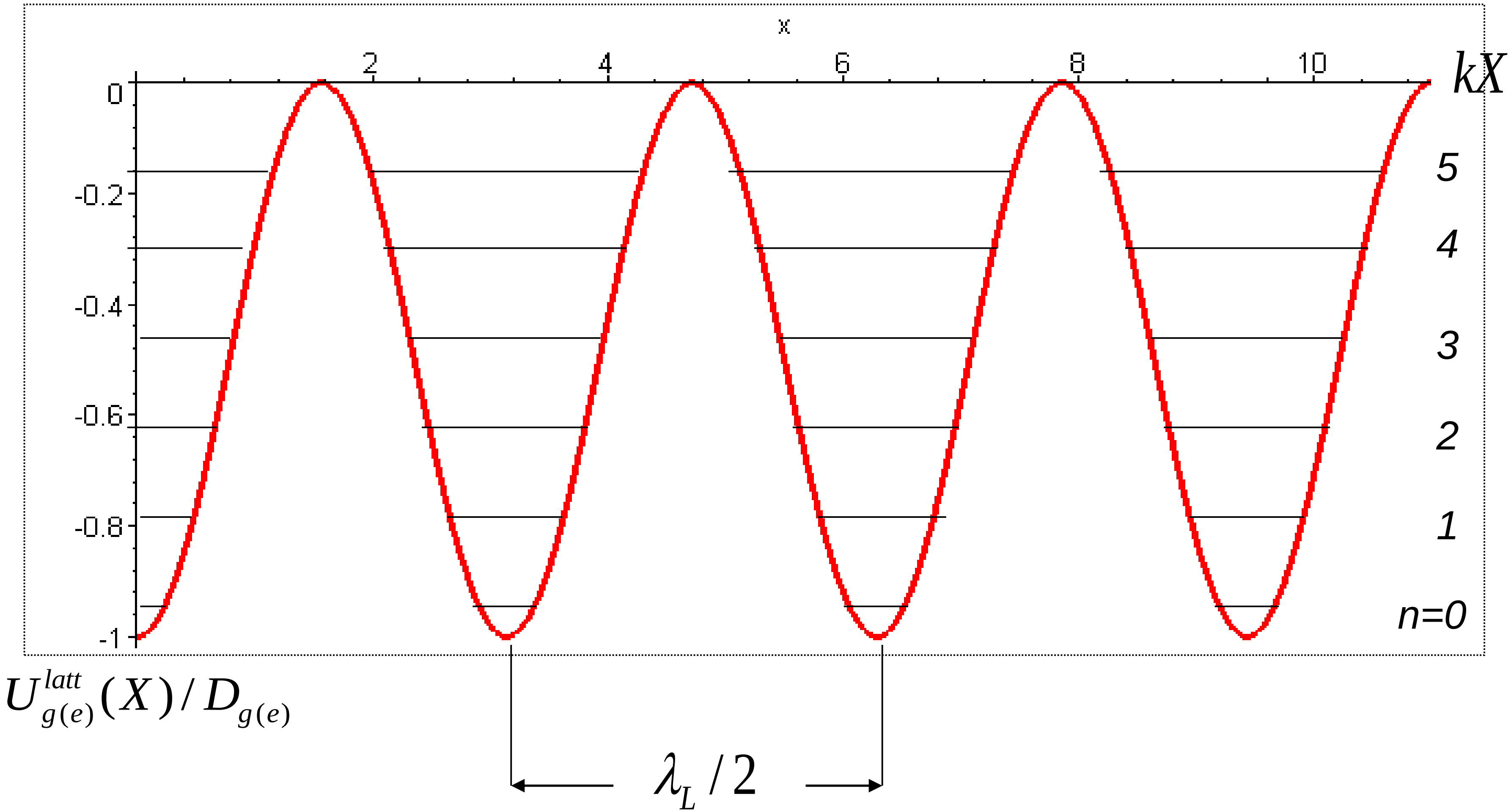

Stark-trap potential and vibration-state energies (in the units of the potential depth $D_{g(e)}$) of an atom in a lattice field

$$\mathrm{E}_{g(e)}^{latt} = \mathrm{E}_{g(e)}^{(0)} + \mathrm{E}_{g(e)}^{vib}(\omega, \xi, I, n); \quad \xi = \sin 2\varepsilon \text{ is the CPD,}$$

$$\varepsilon = \arctan(b/a) \text{ is the ellipticity,} \quad |\varepsilon| \le \pi/4$$

The magic-wavelength (MWL) condition implies the equality

$$\mathrm{E}_{e}^{vib}(\omega_{mag}, \xi, I, n) = \mathrm{E}_{g}^{vib}(\omega_{mag}, \xi, I, n)$$

To hold this condition, the equalities should hold for the following ground-state (g) and excited-state (e) susceptibilities:

$$\alpha_{g(e)}^{E1}(\omega); \qquad \alpha_{g(e)}^{qm}(\omega) = \alpha_{g(e)}^{E2}(\omega) + \alpha_{g(e)}^{M1}(\omega);$$

$$\alpha_{g(e)}^{dqm}(\omega) = \alpha_{g(e)}^{E1}(\omega) - \alpha_{g(e)}^{qm}(\omega);$$

$$\beta_{g(e)}(\xi, \omega) = \beta_{g(e)}^{lin}(\omega) + \xi^2 \left[\beta_{g(e)}^{c}(\omega) - \beta_{g(e)}^{lin}(\omega) \right]; \quad |\xi| \le 1.$$

The most important of which is the E1 polarizability, so the primitive MWL condition implied

$$\alpha_{e}^{E1}(\omega_{mag}) = \alpha_{g}^{E1}(\omega_{mag})$$

The Fues' model-potential approach evaluates the magic wavelength at $\lambda_{mag}^{E1} \approx 471.6$ nm

$-\alpha^{E1}(\lambda)\ \left(\mathrm{kHz/(kW/cm^2)}\right)$

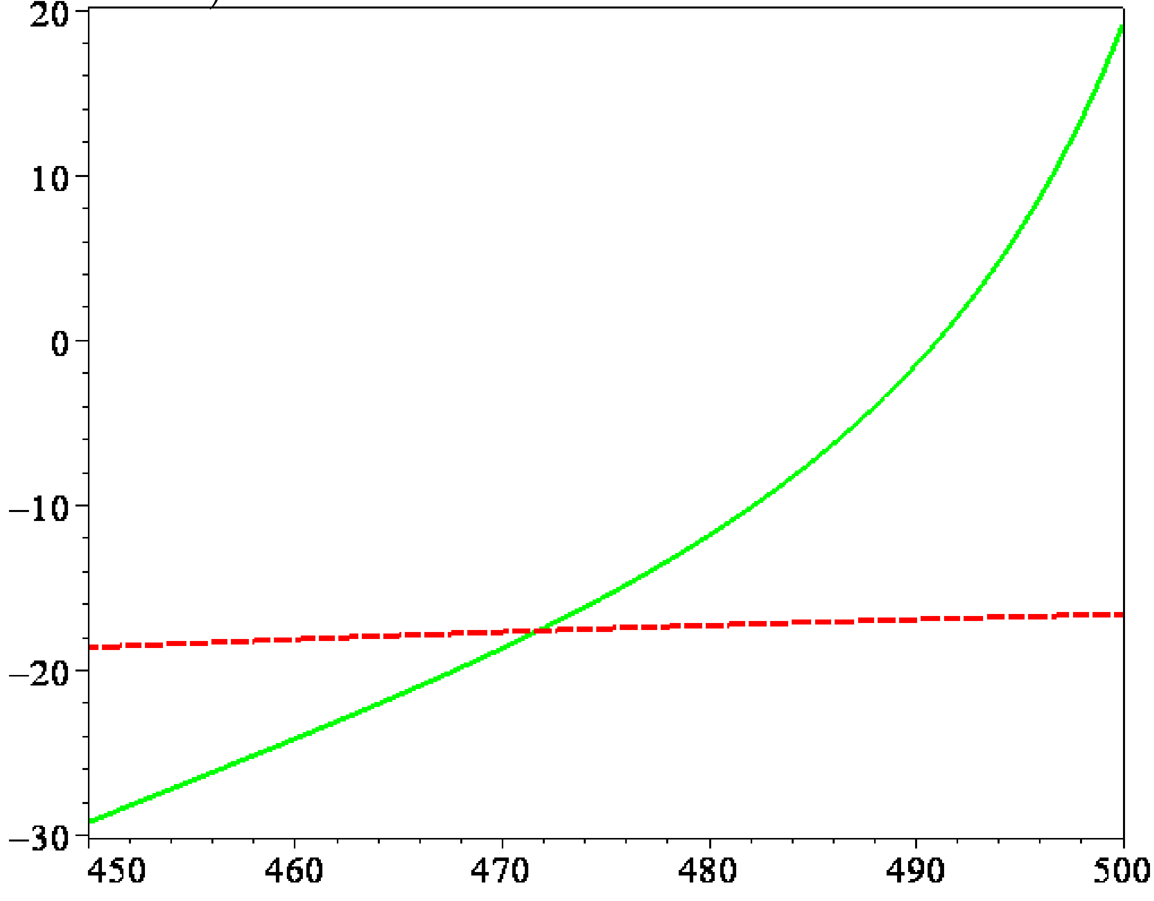

λ (nm)

Dipole polarizabilities of the clock ground (red dashed) and excited (green bold) states of Mg atom

2c) Lattice-induced clock-frequency shift.

$$\nu_{cl}^{latt} = \nu_{cl}^{(0)} + \Delta\nu_{cl}^{latt}; \quad \nu_{cl}^{(0)} = \mathrm{E}_e^{(0)} - \mathrm{E}_g^{(0)}; \quad \Delta\nu_{cl}^{latt} = \mathrm{E}_e^{vib} - \mathrm{E}_g^{vib};$$

$$\Delta\nu_{cl}^{latt} = -\Delta D + \Delta\Omega\left(n + \frac{1}{2}\right) - \Delta\mathrm{E}^{anh}\left(n^2 + n + \frac{1}{2}\right);$$

$$\Delta D = \left[\alpha_e^{E1}(\omega) - \alpha_g^{E1}(\omega)\right] I + \left[\beta_e(\omega) - \beta_g(\omega)\right] I^2;$$

$$\Delta\Omega = \Omega_e - \Omega_g = 2\sqrt{\mathrm{E}^{rec} I}\left[\sqrt{\alpha_e^{dqm}(\omega) + 2\beta_e(\omega) I} - \sqrt{\alpha_g^{dqm}(\omega) + 2\beta_g(\omega) I}\right];$$

$$\Delta\mathrm{E}^{anh} = \frac{3}{2}\mathrm{E}^{rec}\left[\frac{\beta_e(\xi,\omega)}{\alpha_e^{dqm}(\omega)} - \frac{\beta_g(\xi,\omega)}{\alpha_g^{dqm}(\omega)}\right] I$$

$$\Delta \nu_{cl}^{latt}(n,\xi,I) = c_{1/2}(n) I^{1/2} + c_1(n,\xi) I + c_{3/2}(n,\xi) I^{3/2} + c_2(\xi) I^2$$

If $\Delta\beta^{l}(\xi,\omega_{mag}) / \Delta\beta^{c}(\xi,\omega_{mag}) < 0,$

then $\xi_{mag} = \pm 1/\sqrt{1-\Delta\beta^{c}/\Delta\beta^{l}},$

$$\Delta\beta(\xi_{mag},\omega_{mag}) = 0.$$

Assuming the lattice laser frequency $\omega = \omega_{mag}^{E1} + \delta$, where the magic frequency ω_{mag}^{E1}

is determined from equalization of the E1 polarizabilities of the clock states,

$$\alpha_g^{E1}(\omega_{mag}^{E1}) = \alpha_e^{E1}(\omega_{mag}^{E1}) \equiv \alpha_m^{E1}$$

The coefficients for the lattice-induced shift are presented in terms of the clock-state susceptibilities, as follows

$$c_{1/2}^{E1}(n,\delta) = \left(\frac{\partial \Delta\alpha_m^{E1}}{\partial \nu}\delta - \Delta\alpha_{E1}^{qm} \right) \sqrt{\frac{\mathrm{E}_{E1}^{rec}}{\alpha_m^{E1}}} \left(n + \frac{1}{2} \right), \quad c_1^{E1}(\xi,n,\delta) = -\frac{\partial \Delta\alpha_m^{E1}}{\partial \nu}\delta - \frac{3\mathrm{E}_{E1}^{rec}}{2\alpha_m^{E1}} \Delta\beta_{E1}(\xi) \left(n^2 + n + \frac{1}{2} \right),$$

$$c_{3/2}^{E1}(\xi,n) = 2\Delta\beta_{E1}(\xi) \sqrt{\frac{\mathrm{E}_{E1}^{rec}}{\alpha_m^{E1}}} \left(n + \frac{1}{2} \right), \quad c_2^{E1}(\xi) = -\Delta\beta_{E1}(\xi).$$

3. Numerical values of electromagnetic susceptibilities at ω_{mag}^{E1}

The constant in the last line gives the value of the BBR-induced shift: $\Delta\nu^{BBR}(T)=\nu_0^{BBR}\cdot(T/300\text{ K})^4$

Table 1

Atom	Mg	Ca	Sr	Yb	Zn	Cd	Hg
λ_{mag}(nm)	**468.46**	747	**813.43**	**759.36**	406.5	414.4	**362.57**
$\nu_{clock}\,(\text{THz})$	655	455	429	518	969	903	1129
$\alpha_m^{E1}\left(\frac{\text{kHz}}{\text{kW/cm}^2}\right)$	17.5	48.0	45.2	40.5	8.11	9.76	5.70
$\Delta\alpha_m^{qm}\left(\frac{\text{mHz}}{\text{kW/cm}^2}\right)$	5.48	– 2.0	– 6.20	– 8.06	15.3	5.86	8.25
$\Delta\beta_m^{l}\left[\frac{\mu\text{Hz}}{(\text{kW/cm}^2)^2}\right]$	111+ 5.88i	497	– 200.0	– 312	– 4.3 +1.64i	– 5.47 +2.02i	– 2.67 +0.82i
$\Delta\beta_m^{c}\left[\frac{\mu\text{Hz}}{(\text{kW/cm}^2)^2}\right]$	1735+ 8.69i	1024	– 311.0	238	42.6 +2.45i	19.5 +3.01i	0.94 +1.21i
$\frac{\Omega_m}{\sqrt{I}}\left[\frac{\text{kHz}}{\sqrt{\text{kW/cm}^2}}\right]$	51.5	41.4	25.05	18.0	24.1	19.9	13.1
$\frac{\partial\left(\Delta\alpha_m^{E1}\right)}{\partial\nu}\left(\frac{10^{-9}}{\text{kW/cm}^2}\right)$	0.420	0.273	0.254	0.720	0.187	0.200	0.134
$\text{E}^{rec}\,(\text{kHz})$	37.9	8.94	3.47	2.00	17.9	10.14	7.57
$\nu_0^{BBR}\,(\text{Hz})$	– 0.424	– 0.64	**– 2.13**	**– 1.25**	– 0.23	– 0.22	– 0.188

Coefficients for the lattice-induced shift dependence on the laser intensity

Table 2

ATOM	Mg	Sr	Yb	Hg
$c_{1/2}$, mHz(kW/cm^2)$^{-1/2}$	–4.03	0.86	0.19	– 4.75
c_1 $(\xi=0)$, mHz(kW/cm^2)$^{-1}$	– 0.18 – 0.0096i	0.0115	0.0116	0.00266 – 0.00082i
c_1 $(\xi=\pm1)$, mHz(kW/cm^2)$^{-1}$	– 2.82 – 0.0141i	0.0179	-0.0088	–0.000936 – 0.00121i
$c_{3/2}$ $(\xi=0)$, mHz(kW/cm^2)$^{-3/2}$	0.163 + 0.0087i	– 0.055	–0.069	–0.00308 + 0.00095i
$c_{3/2}$ $(\xi=\pm1)$, mHz(kW/cm^2)$^{-3/2}$	2.55 + 0.0128i	– 0.086	0.053	0.00108 + 0.00139i
c_2 $(\xi=0)$, mHz(kW/cm^2)$^{-2}$	– 0.111 – 0.006i	0.20	0.312	0.00267 – 0.00082i
c_2 $(\xi=\pm1)$, mHz(kW/cm^2)$^{-2}$	– 1.73 – 0.0087i	0.311	–0.238	–0.00094 – 0.00121i

Dependence on the lattice-laser intensity of the clock-frequency shift in Mg atoms for positive (a) and negative (b) detuning of the laser frequency from the magic frequency ω_{mag}^{E1}

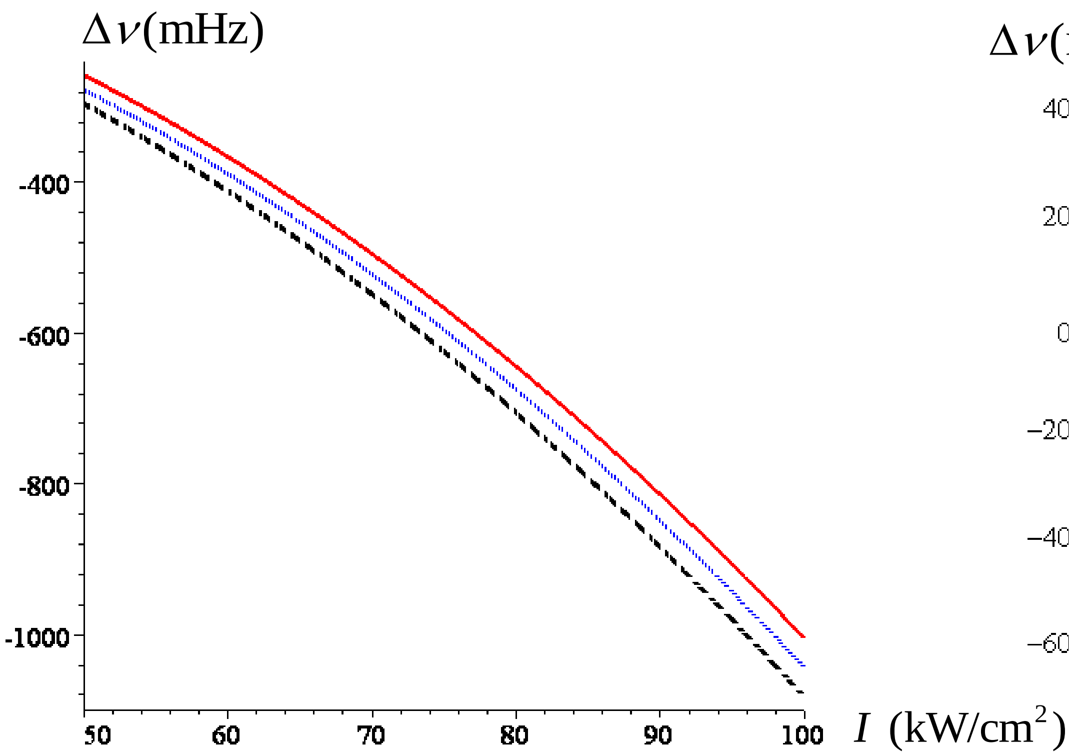

(a): $\delta = 0$ (red solid), 1 MHz (blue dotted) and 2 MHz (black dashed line)

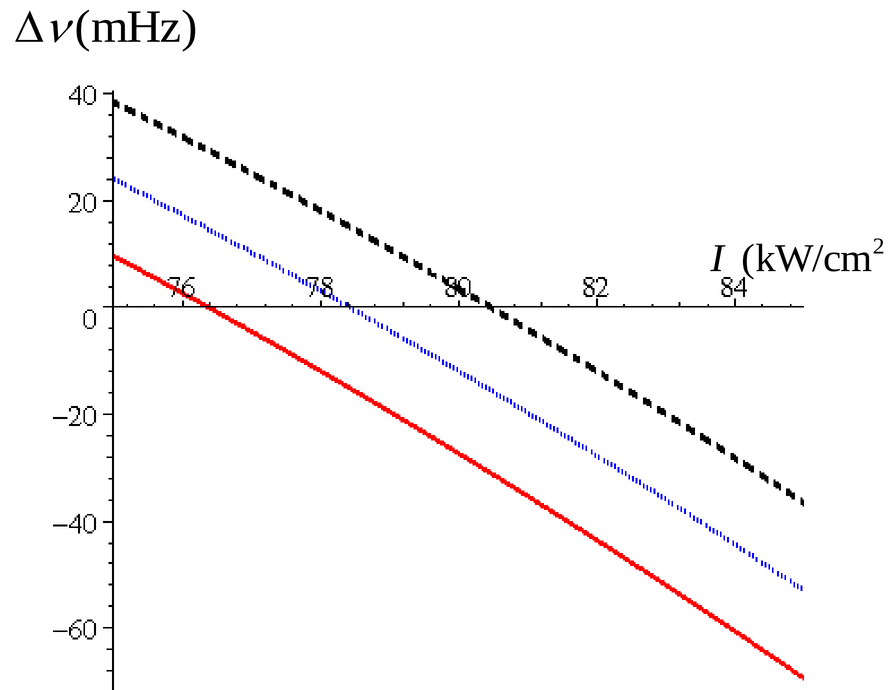

(b): $\delta = -20$ (red solid), -20.5 MHz (blue dotted) and -21 MHz (black dashed line)

Dependence on the lattice-laser intensity of the clock-frequency shift in Mg atoms at a most appropriate detuning $\delta = \omega - \omega_{mag}^{E1}$ for ensuring the least deviations of the shift

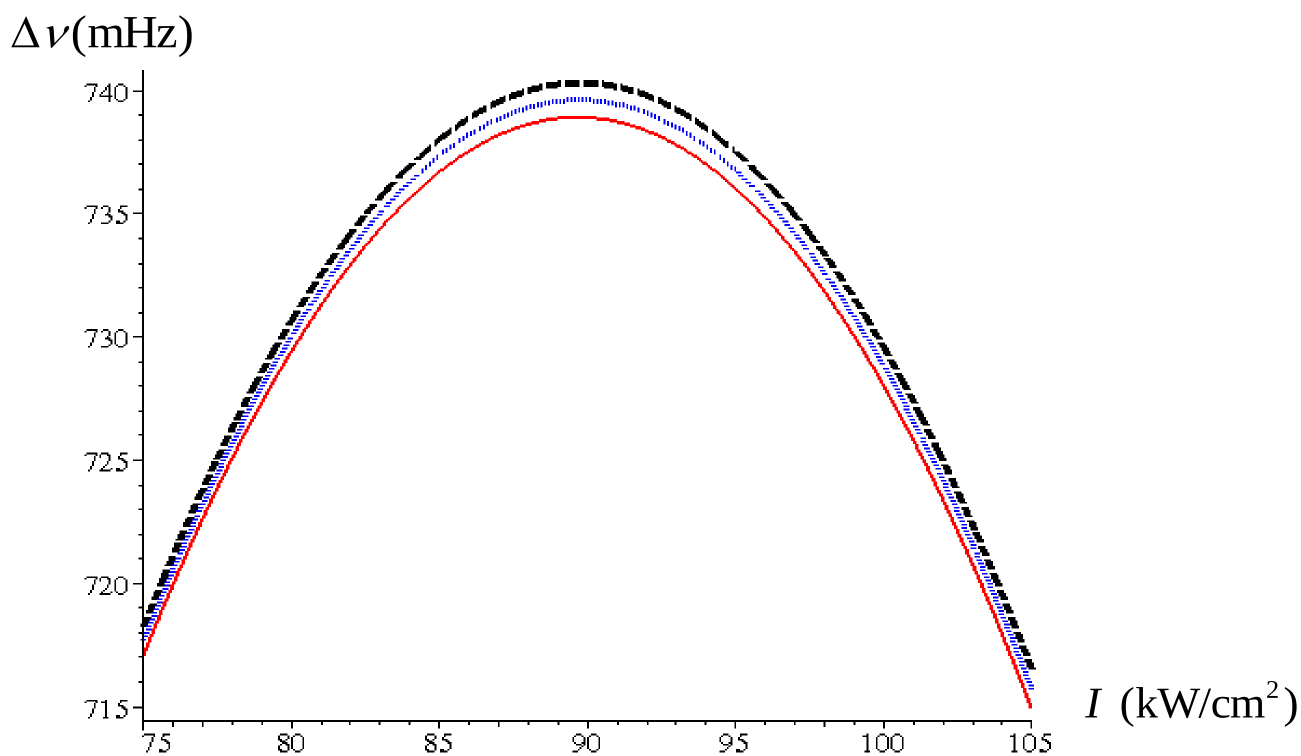

$\delta = -44.54$ (red solid), $\delta = -44.56$ (blue dotted)
and $\delta = -44.58$ MHz (black dashed line)

Dependence on the intensity of magic-elliptically polarized lattice-laser radiation of the clock-frequency shift in Hg atoms for a negative (b) detuning $\delta = \omega - \omega_{mag}^{E1}$ of the laser frequency ω from the magic frequency ω_{mag}^{E1}

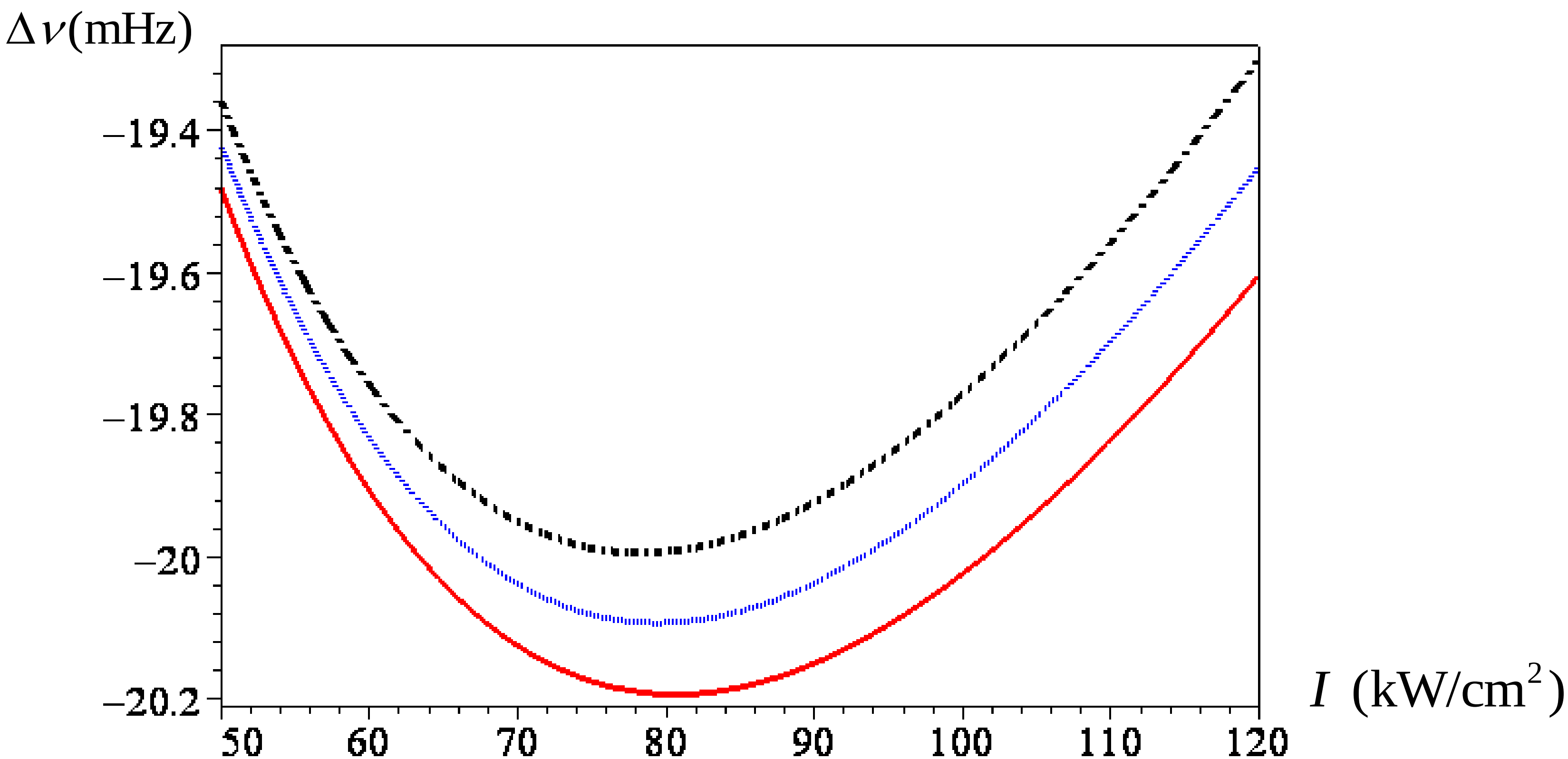

$\delta = -2.41$ (red solid), $\delta = -2.42$ (blue dotted)

and $\delta = -2.43$ MHz (black dashed line)

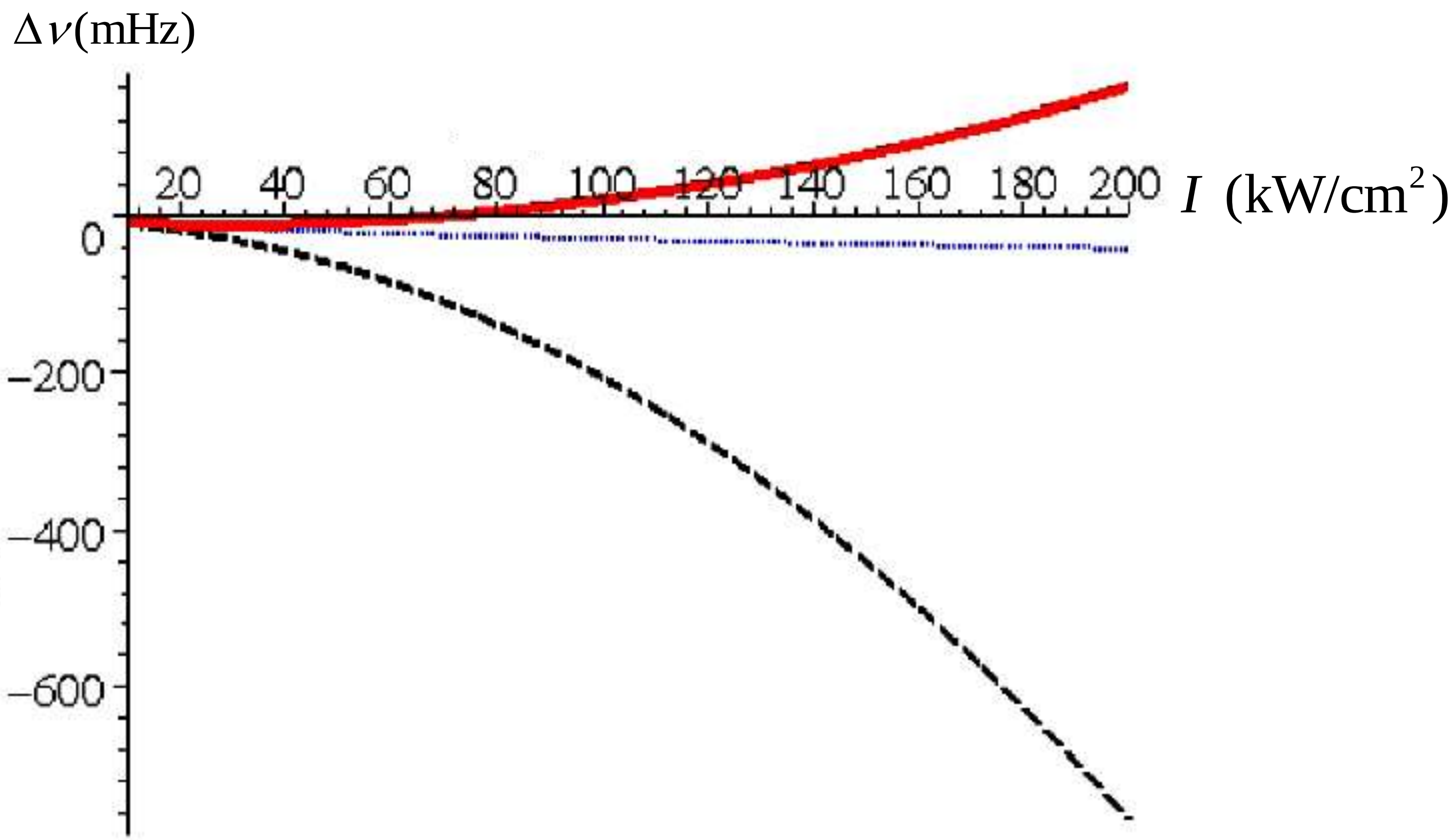

The clock-frequency shift of Cd atoms as a function of the lattice-laser intensity for linear (red bold line), magic elliptical (blue dotted) and **circular (black dashed)** polarization of the lattice-laser wave

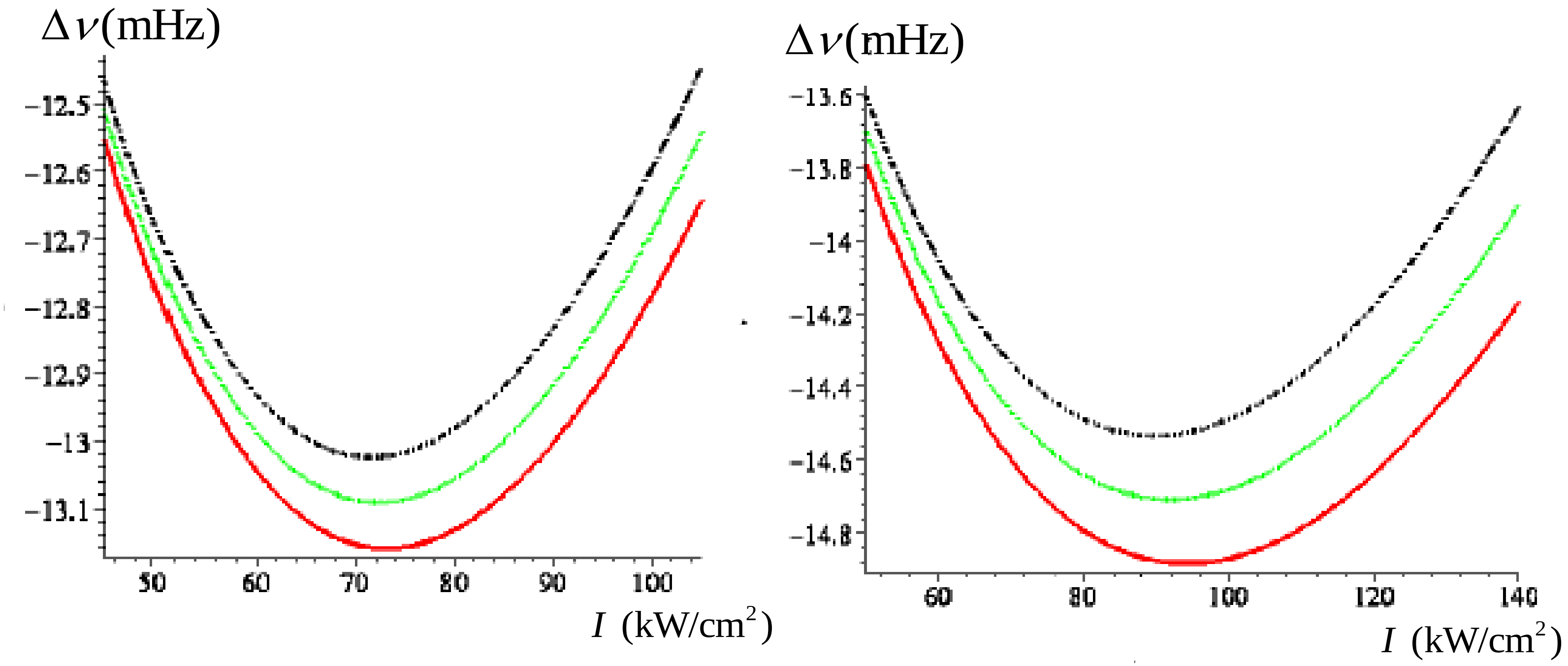

(a) (b)

The clock-frequency shift of Cd atoms as a function of the lattice-laser intensity for the magic elliptical polarization of the laser wave and the laser-frequency detuning from ω_{mag}^{E1} :

(a) $\delta = -$ 900 (red solid curve), $\delta = -$ 905 (green dotted) and $\delta = -$ 910 kHz **(black dash-dotted)**;

(b) $\delta = -$ 790 (red solid curve), $\delta = -$ 800 (green dotted) and $\delta = -$ 810 kHz **(black dash-dotted)**.

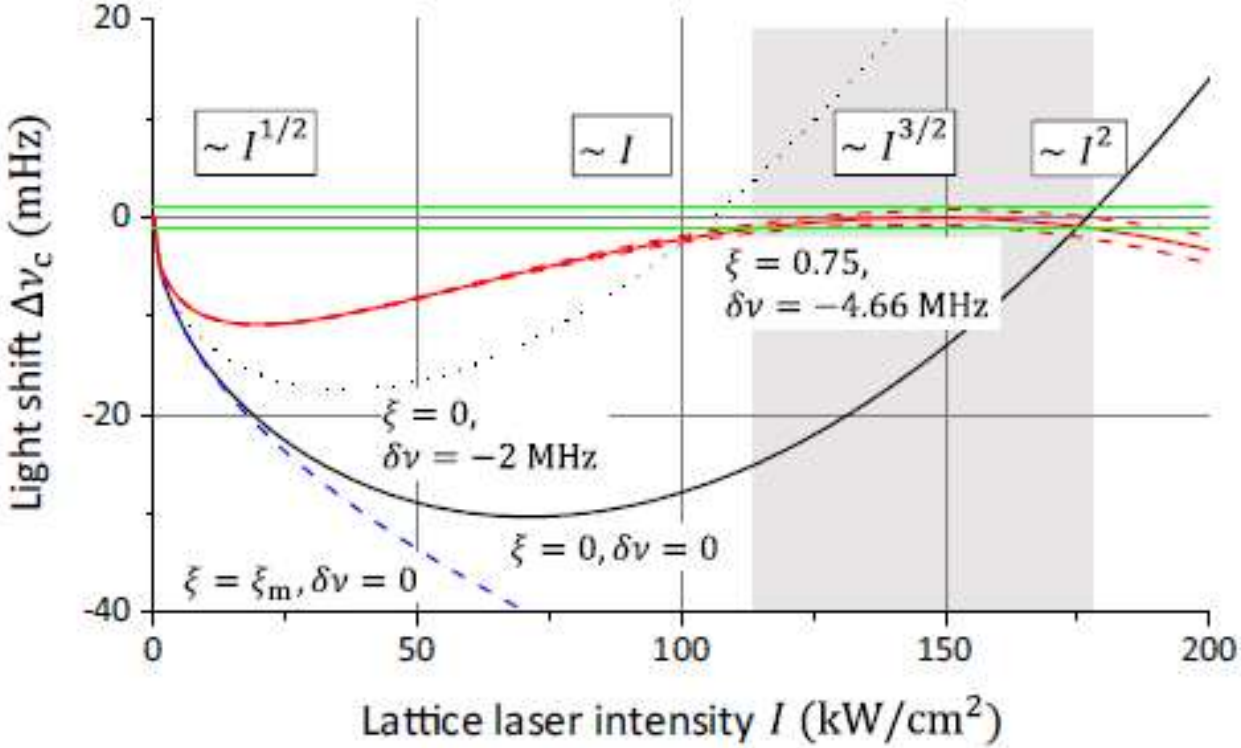

FIG. 3. (Color online) Light shift for a Hg clock as a function of laser intensity I. The black solid and blue dashed lines correspond to linear-polarized and "magic-elliptical" light with detuning $\delta\nu = 0$. With $\delta\nu = -4.66$ MHz and $\xi^{\mathrm{Hg}} = 0.75$, the light shift (red solid line) becomes less than ± 1 mHz (green) for the gray shaded region. The red dashed lines indicate the tolerance (0.5%) for ξ^{Hg}. For linear polarized light ($\xi = 0$) with $\delta\nu = -2$ MHz, the light shift becomes insensitive to ΔI around $I \sim 36$ kW/cm^2 (dotted line).

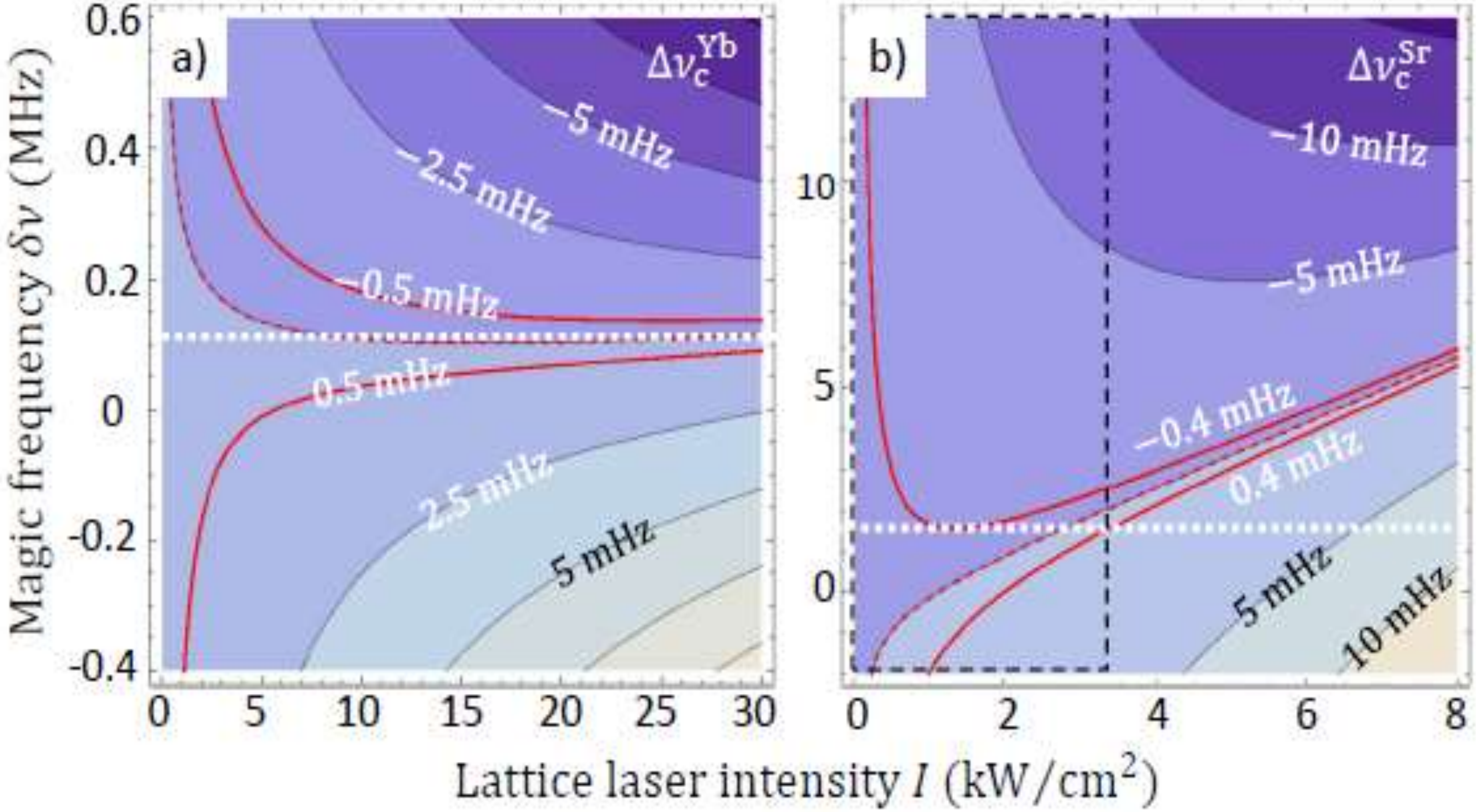

FIG. 4. Contour plots of light shifts for a) Yb and b) Sr clock transitions as functions of lattice laser intensity I and detuning $\delta\nu$, for $\xi^{\mathrm{Yb}} = 0.75$ and $\xi^{\mathrm{Sr}} = 0$. The red-dotted lines show zero light shift. The region bound by red lines corresponds to light shift $|\Delta\nu_{\mathrm{c}}|/\nu_0 \leq 1\times10^{-18}$. Tuning to the operational magic frequency $\delta\nu$ as indicated by white dotted lines, wide range of operational intensities are allowed.

Thanks for your attention!